

ARTICLE OPEN

Oxidation stability of $\text{Ti}_3\text{C}_2\text{T}_x$ MXene nanosheets in solvents and composite filmsTouseef Habib¹, Xiaofei Zhao¹, Smit A. Shah¹, Yexiao Chen², Wanmei Sun¹, Hyosung An¹, Jodie L. Lutkenhaus^{1,2}, Miladin Radovic² and Micah J. Green^{1,2}

$\text{Ti}_3\text{C}_2\text{T}_x$ belongs to the family of MXenes, 2D materials with an attractive combination of functional properties suitable for applications such as batteries, supercapacitors, and strain sensors. However, the fabrication of devices and functional coatings based on $\text{Ti}_3\text{C}_2\text{T}_x$ remains challenging as they are prone to chemical degradation by their oxidation to TiO_2 . In this paper, we examine the oxidation of $\text{Ti}_3\text{C}_2\text{T}_x$ in air, liquid, and solid media via conductivity measurements to assess the shelf life of $\text{Ti}_3\text{C}_2\text{T}_x$ MXenes. The oxidation of $\text{Ti}_3\text{C}_2\text{T}_x$ was observed in all the media used in this study, but it is fastest in liquid media and slowest in solid media (including polymer matrices). We also show that the conventional indicators of MXene oxidation, such as changes in color and colloidal stability, are not always reliable. Finally, we demonstrate the acceleration of oxidation under exposure to UV light.

npj 2D Materials and Applications (2019)3:8; <https://doi.org/10.1038/s41699-019-0089-3>

INTRODUCTION

MXenes are 2D materials consisting of M (early transitional metal), X (carbon or nitrogen), and T (terminal groups). MXenes can be represented with the general formula $M_{n+1}X_nT_x$, where $n = 1, 2, 3$ and x represents the number of terminal groups. They are commonly derived from the parent MAX (or $M_{n+1}AX_n$) phases by the selective etching of the A element (a group-13 or -14 element). Out of over 70 known MAX phases with different compositions, only a few (~20) have actually been experimentally converted into MXenes.^{1,2} The most common type of MXenes are titanium carbides ($\text{Ti}_3\text{C}_2\text{T}_x$), which are obtained from the parent titanium aluminum carbide (Ti_3AlC_2) MAX phase by the removal of the aluminum layer by etching in hydrofluoric acid or in a mixture of HCl and fluoride salts; however, there is a research interest in pursuing etching without the use of fluoride ions.^{1,3} $\text{Ti}_3\text{C}_2\text{T}_x$ possesses high electrical conductivity, excellent electromagnetic shielding properties, and a high in-plane stiffness.^{4–8}

The terminal groups (such as -F, -OH, and =O) of $\text{Ti}_3\text{C}_2\text{T}_x$ MXenes are polar, making them hydrophilic and suitable for processing in water without the need of a dispersant. Aqueous $\text{Ti}_3\text{C}_2\text{T}_x$ nanosheet dispersions can be assembled into films, polymer composites, or even into 3D crumpled morphologies.^{9–11} These MXene-based bulk materials have been utilized for hydrogen storage, antibacterial films, flexible electronics, water desalination, and absorption of heavy metals.^{12–16} Additionally, because of their high conductivity and ease of processing, there is substantial research interest in utilizing these materials for batteries, supercapacitors, and strain sensors.^{8,17–23}

Despite the promising properties of MXenes, questions about their chemical stability linger. Although a number of reports do not mention this, $\text{Ti}_3\text{C}_2\text{T}_x$ MXenes are known to oxidize over time. This hampers the utility of $\text{Ti}_3\text{C}_2\text{T}_x$ (and other MXenes) in numerous applications. Only a few prior studies have explored

this problem, but methods for preventing or delaying the oxidation of MXenes are still not well understood. Ghassemi et al. demonstrated the controlled oxidation of $\text{Ti}_3\text{C}_2\text{T}_x$ MXenes under air to obtain TiO_2 by varying the heating rate, temperature range, and exposure time and showed that slow heating rates cause the formation of rutile TiO_2 particles whereas quick heating rates result in the formation of anatase TiO_2 particles. The formation of TiO_2 grains was observed through transmission electron microscopy.²⁴ Halim et al. observed oxidation on the surfaces of air-aged free-standing disks made by cold pressing various multilayer MXene nanosheets ($\text{Ti}_3\text{C}_2\text{T}_x$, Ti_2CT_x , Ti_3CNT_x , Nb_2CT_x , and $\text{Nb}_4\text{C}_3\text{T}_x$). The authors observed an increase in oxygen content on the surface with time.²⁵ Maleski et al. dispersed $\text{Ti}_3\text{C}_2\text{T}_x$ in a wide range of organic solvents (polar protic, polar aprotic, and nonpolar) and analyzed the colloidal dispersion quality using Hildebrand and Hansen solubility theory. The authors noted that the color of $\text{Ti}_3\text{C}_2\text{T}_x$ in water dispersion changed from black to white, whereas that in organic solvent dispersions stayed black ($\text{Ti}_3\text{C}_2\text{T}_x$ MXenes are generally black and TiO_2 particles are white). They proposed that the lack of color change indicates a slower oxidation rate in organic solvents when compared to water, suggesting the reaction of water molecules with $\text{Ti}_3\text{C}_2\text{T}_x$.²⁶ Zhang et al. studied the degradation of MXene flakes in aqueous solutions and reported the following: (i) the degradation of MXene flakes is size-dependent, (ii) the decreasing colloidal stability is correlated with MXene oxidation, and (iii) an oxidation-preventive storage method: storing MXene–water dispersions in hermetically sealed Argon-filled vials at 5 °C. The authors suggest that the dissolved oxygen in MXene dispersion plays a role in oxidation.²⁷

Despite these efforts, our current understanding of the comparative oxidation of MXenes in different media and conditions remains elusive. In this paper, we examine the oxidation of $\text{Ti}_3\text{C}_2\text{T}_x$ in air, liquid (water, acetone, and acetonitrile),

¹Artie McFerrin Department of Chemical Engineering, Texas A&M University, College Station, TX 77845, USA and ²Materials Science & Engineering Department, Texas A&M University, College Station, TX 77845, USA

Correspondence: Miladin Radovic (mradovic@tamu.edu) or Micah J. Green (micah.green@tamu.edu)

Received: 29 April 2018 Accepted: 6 January 2019

Published online: 13 February 2019

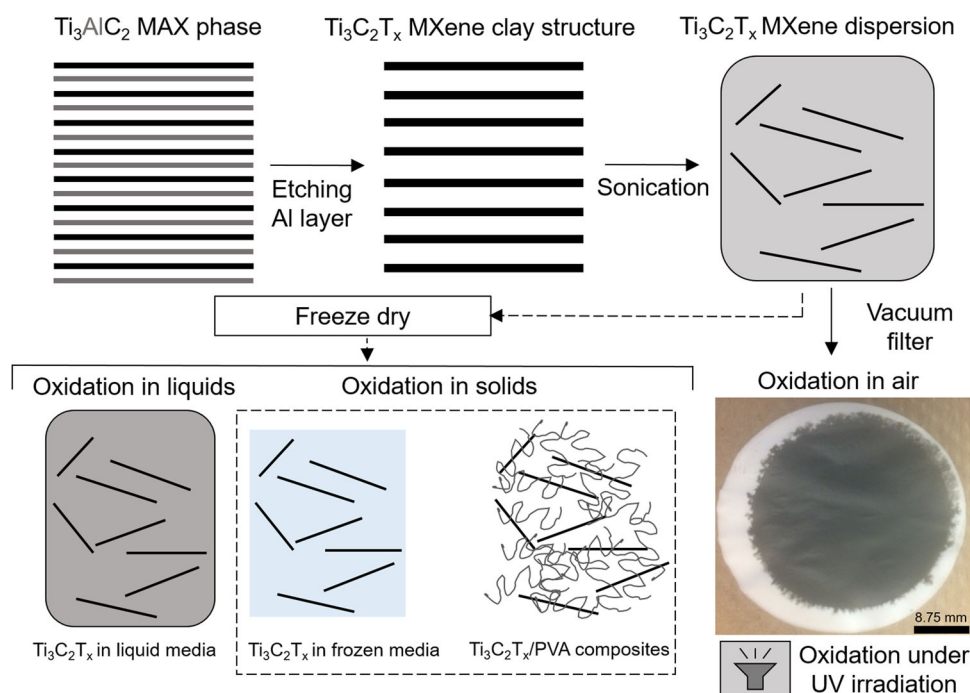


Fig. 1 An overview of the experimental procedure: after the synthesis of $\text{Ti}_3\text{C}_2\text{T}_x$ MXene nanosheets from parent MAX phases, the samples were dispersed in various media

and solid (ice and polymer) media to understand how storage and/or dispersion media influence $\text{Ti}_3\text{C}_2\text{T}_x$ oxidation processes. Under air, we observe a continual decrease in conductivity with a longer exposure time. In aqueous dispersions, we observe a sharp decrease in electrical conductivity while the dispersion retains its dark color and colloidal stability even when the majority of it is oxidized. $\text{Ti}_3\text{C}_2\text{T}_x$ dispersed in organic solvents (acetone and acetonitrile) had a sharp drop in conductivity after being aged 14 days in each medium. In air and solid media (frozen samples and polymer composites), the drop in conductivity was slower than that in liquid media.

RESULTS

To prepare $\text{Ti}_3\text{C}_2\text{T}_x$ MXene clay, we followed a previously reported procedure for etching the A layer from the parent Ti_3AlC_2 (MAX phase) in a mixture of LiF and HCl for 45 h.^{11,28} After etching, the $\text{Ti}_3\text{C}_2\text{T}_x$ (MXene) clay was washed with deionized (DI) water. The $\text{Ti}_3\text{C}_2\text{T}_x$ powder was intercalated with dimethyl sulfoxide (DMSO) and then solvent exchanged to water. The $\text{Ti}_3\text{C}_2\text{T}_x$ MXene in water was bath sonicated and centrifuged, and the supernatant of dispersed, delaminated $\text{Ti}_3\text{C}_2\text{T}_x$ nanosheets was collected. These dispersions were freeze dried to obtain $\text{Ti}_3\text{C}_2\text{T}_x$ nanosheets, which were used to prepare samples by re-dispersing them in liquids (DI water, acetone, and acetonitrile) and in solid media (ice and polymer matrices). The experimental procedure is schematically depicted in Fig. 1.

We used the electrical conductivity of vacuum-filtered MXene films as an indicator of the degree of oxidation in air. Prior studies have shown that an increased oxygen content in titanium oxide films leads to lower conductivity; similar trends also exist for graphene conductivity and oxidation.^{29–31} After delamination, aqueous dispersions of $\text{Ti}_3\text{C}_2\text{T}_x$ nanosheets were vacuum filtered to obtain a $\text{Ti}_3\text{C}_2\text{T}_x$ nanosheet buckypaper. The buckypaper was vacuum dried overnight to remove any excess moisture, and its electrical conductivity was measured to be $2.49 \times 10^4 \pm 1.16 \times 10^3 \text{ S m}^{-1}$; this was used as a starting conductivity value for studying $\text{Ti}_3\text{C}_2\text{T}_x$ oxidation in air and water. The buckypaper was kept at

room temperature for the duration of the experiment, and its electrical conductivity was measured over time. Over a period of 2 months, these $\text{Ti}_3\text{C}_2\text{T}_x$ vacuum-filtered films exposed to atmospheric air displayed a strong decrease in conductivity (Fig. 2a). After 27 days of exposure, the conductivity was roughly 7% of the original value of $2.49 \times 10^4 \pm 1.16 \times 10^3 \text{ S m}^{-1}$, suggesting rapid oxidation. The conductivity on the 64th day was $4.90 \times 10^2 \text{ S m}^{-1}$, which was less than 2% from the original 0th day measurement. This suggests a strong decrease in conductivity between the 0th and 27th day, and a weaker rate of decrease thereafter. In other words, the sample had more reactive sites in the early stages of the experiment such that the oxidation occurs much faster. As the number of reactive sites decreases with time, the oxidation rate becomes slower. The fluctuations on the later days (27th day onwards) can be attributed to changes in air humidity since humidity has been shown to affect the electrical conductivity of $\text{Ti}_3\text{C}_2\text{T}_x$ MXenes.³²

For our study of oxidation in liquid media, three solvents (water, acetone, and acetonitrile) were used. We chose acetone and acetonitrile because non-delaminated MXenes were observed to be the most resistant in these solvents (Supplementary Figs S5 and S6). The freeze-dried $\text{Ti}_3\text{C}_2\text{T}_x$ nanosheet powder was re-dispersed in all the three liquid solvents at a concentration of 1 mg ml^{-1} using a vortex mixer. The freeze-dried powder dispersed back in water forming a colloidal dispersion but it did not disperse in acetone and acetonitrile. All the samples were prepared on the same day.

We will first discuss the oxidation of $\text{Ti}_3\text{C}_2\text{T}_x$ in aqueous dispersions (Table 1). After storing MXenes in water for 1 week, a portion of the dispersion was vacuum filtered into a film and its electrical conductivity was measured; the conductivity of the MXene sample dropped from $2.49 \times 10^4 \pm 1.16 \times 10^3 \text{ S m}^{-1}$ to $8.52 \times 10^3 \pm 1.21 \times 10^3 \text{ S m}^{-1}$, or by more than 65% compared to the original sample. After 14 days, a portion of the remaining dispersion (supernatant) was again vacuum filtered into a film and its conductivity was measured. The conductivity of this MXene buckypaper was below the measurement threshold ($<10^3 \text{ S m}^{-1}$), suggesting a significant oxidation of $\text{Ti}_3\text{C}_2\text{T}_x$. The results are in

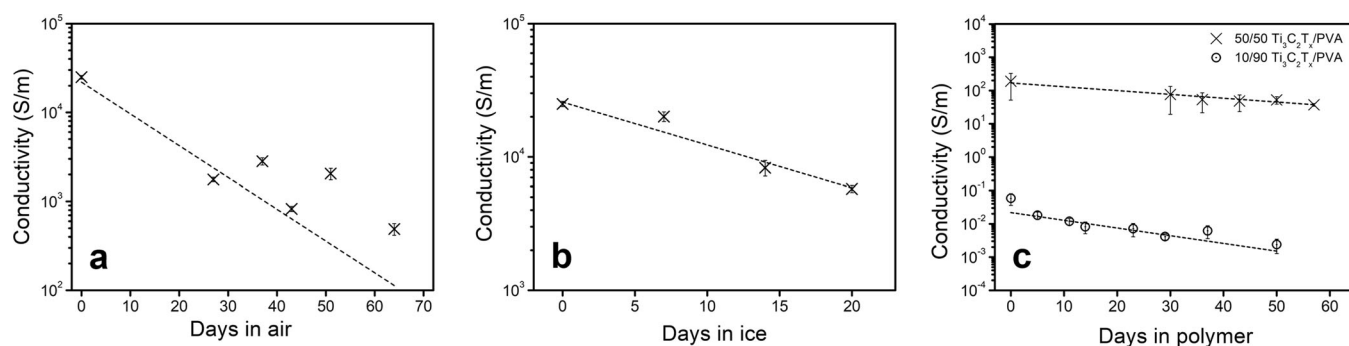


Fig. 2 Conductivity vs time measurements with error bars (standard deviations) for **a** $\text{Ti}_3\text{C}_2\text{T}_x$ films in air, **b** films made from aged $\text{Ti}_3\text{C}_2\text{T}_x$ dispersed in ice, and **c** $\text{Ti}_3\text{C}_2\text{T}_x$ /PVA composite films. The decrease in conductivity is indicative of increasing oxidation

Table 1. Conductivity (S m^{-1}) of films made from aqueous MXene dispersions with varying dispersion age

	Day 0	Day 7	Day 14
Water	$2.5 \pm 0.1 \times 10^4$	$8.5 \pm 1.2 \times 10^3$	$< 10^{-3}$
Acetone	$7.9 \pm 3.7 \times 10^3$	$2.4 \pm 0.9 \times 10^2$	$4.0 \pm 0.6 \times 10^1$
Acetonitrile	$3.0 \pm 0.2 \times 10^3$	$1.3 \pm 0.1 \times 10^2$	$9.6 \pm 0.5 \times 10^1$

agreement with prior literature; Zhang et al. has also reported the complete oxidation of their $\text{Ti}_3\text{C}_2\text{T}_x$ MXene dispersion within a span of 2 weeks.²⁷ Their claim was based on a drop in ultraviolet (UV) absorbance while ours is based on a drop in conductivity. Although our water- $\text{Ti}_3\text{C}_2\text{T}_x$ system was (initially) a stable colloidal dispersion and black in color (Supplementary Fig. S1), UV-visible (UV-vis) measurements (Supplementary Fig. S2) revealed a massive drop in concentration to 0.2 mg ml^{-1} from the original 1 mg ml^{-1} . The remaining stable colloidal particles had a ζ potential of -25.1 mV , indicative of a strong electrostatic repulsion between the dispersed particles. This suggests that the $\text{Ti}_3\text{C}_2\text{T}_x$ colloidal particles may be oxidized but not to the extent that they become colloidal unstable. X-ray photoelectron spectroscopy (XPS) analysis revealed a high TiO_2 content of 55.8%, confirming oxidation (Supplementary Fig. S3). These data collectively suggest that $\text{Ti}_3\text{C}_2\text{T}_x$ colloidal stability and black color are not always directly correlated with the degree of oxidation.^{26,27}

In addition to investigating the chemical stability of $\text{Ti}_3\text{C}_2\text{T}_x$ in aqueous dispersions, we also investigated the effects of humidity on the chemical stability of $\text{Ti}_3\text{C}_2\text{T}_x$ buckypaper. The $\text{Ti}_3\text{C}_2\text{T}_x$ buckypaper samples were stored in three different relative humidity (RH) conditions: 0, 50, and 80%. The conductivity of these samples was measured and the results are shown in Supplementary Fig. S7a. The samples stored in a dry condition (RH 0%) maintained their conductivity well over a span of 3 weeks, while the samples stored in humid conditions experienced significant drops in conductivity. The wettest sample kept in RH 80% experienced the highest drop in conductivity; the increase in TiO_2 content in this sample correlates well with the decrease in conductivity as shown in Supplementary Fig. S7b.

The freeze-dried $\text{Ti}_3\text{C}_2\text{T}_x$ powder formed a temporary stable colloidal dispersion in acetone and acetonitrile (Supplementary Fig. S8) after vortex mixing even though the $\text{Ti}_3\text{C}_2\text{T}_x$ powder did sediment out after a few minutes. Vacuum-filtered films were prepared by vacuum filtering the temporary dispersions right after vortex mixing (results in Table 1). By day 14, $\text{Ti}_3\text{C}_2\text{T}_x$ aged in all three of the solvents experienced a similar drop in conductivity. However, by day 21, samples prepared from aging in each acetone and acetonitrile possessed a higher conductivity than the sample prepared from water. This indicates that $\text{Ti}_3\text{C}_2\text{T}_x$ oxidation in acetone and acetonitrile occurs at a lower rate than in water.

The continued oxidation in acetone and acetonitrile can be attributed to their hygroscopicity. It is probable that they (acetone and acetonitrile) absorbed and retained water during the experiment. $\text{Ti}_3\text{C}_2\text{T}_x$ MXenes also have a high affinity for water molecules, such that any water present in the atmosphere and/or the solvents would interact with the nanosheets and contribute to oxidation over time.³³ Overall, our data suggest that storing MXenes in liquid media is conducive to oxidation.

Oxidation in ice was assessed by first dispersing $\text{Ti}_3\text{C}_2\text{T}_x$ in water and then freezing it below 0°C . The ice samples were thawed by keeping the vials in room-temperature water for 20 min. Post thawing, the samples were vacuum filtered to obtain buckypaper; the buckypaper was vacuum dried overnight to remove any excess moisture and then its electrical conductivity was measured. The electrical conductivity (as seen in Fig. 2b) compared to the original was, and 23% over 7, 14, and 21 days, respectively (in comparison, Zhang et al. reported a 43% drop in MXene concentration in the fresh sample after 25 days in their system in which the samples were kept at 5°C and pressurized under Argon; presumably, the drop in concentration is the result of the MXenes sedimenting out). Overall, the frozen samples retained the electrical conductivity (within the same order of magnitude) quite well compared to the samples in liquid medium, indicating slower oxidation. The slower oxidation can be attributed to the slower kinetics due to the solid media and lower temperature. $\text{Ti}_3\text{C}_2\text{T}_x$ MXenes in solid media display slower oxidation rates. Even so, the oxidation process cannot be entirely prevented.

$\text{Ti}_3\text{C}_2\text{T}_x$ has also shown its potential as a filler in polymers with enhanced electrical conductivity, mechanical performance, and electromagnetic interference shielding performance.^{5,6,10,14,34} However, no studies have explored any decrease in performance of these materials due to $\text{Ti}_3\text{C}_2\text{T}_x$ nanosheet oxidation. This issue is critical because of the potential commercial applications of these $\text{Ti}_3\text{C}_2\text{T}_x$ /polymer composites. If MXene/polymer composites degrade over a short time scale (1–3 weeks), then the long-term utility of such materials becomes compromised, especially for materials that rely on electrical conductivity.

To assess the degradation of MXenes in polymer composites, we synthesized $\text{Ti}_3\text{C}_2\text{T}_x$ /polyvinyl alcohol (PVA) composites and measured the decrease in electrical conductivity with time (Fig. 2c). PVA is a water-soluble polymer with a repeat unit of $[\text{CH}_2\text{CH}(\text{OH})]_n$. It is widely used commercially because of its hydrophilicity, biodegradability, and non-toxicity.³⁵ The freeze-dried $\text{Ti}_3\text{C}_2\text{T}_x$ nanosheet powder was used to prepare these vacuum-filtered polymer composites at the following ratios: (1) 50–50 wt% $\text{Ti}_3\text{C}_2\text{T}_x$ to PVA respectively and (2) 10–90 wt% $\text{Ti}_3\text{C}_2\text{T}_x$ to PVA respectively; both samples were kept under atmospheric conditions for the duration of the experiment. The conductivity of 50–50 wt% $\text{Ti}_3\text{C}_2\text{T}_x$ /PVA sample was roughly 40% of its original value on the 30th day and 20% of the original value by the 57th day. The conductivity of 10–90 wt% $\text{Ti}_3\text{C}_2\text{T}_x$ /PVA sample was roughly 7% of

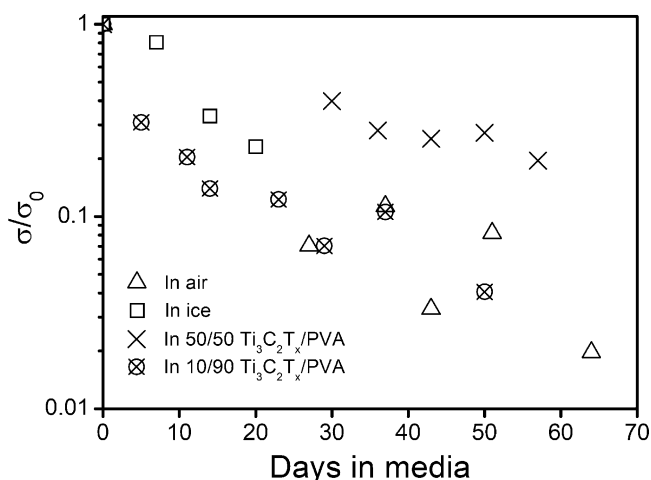


Fig. 3 Master curve for the normalized conductivity variation of films made from MXenes dispersed in various media over time

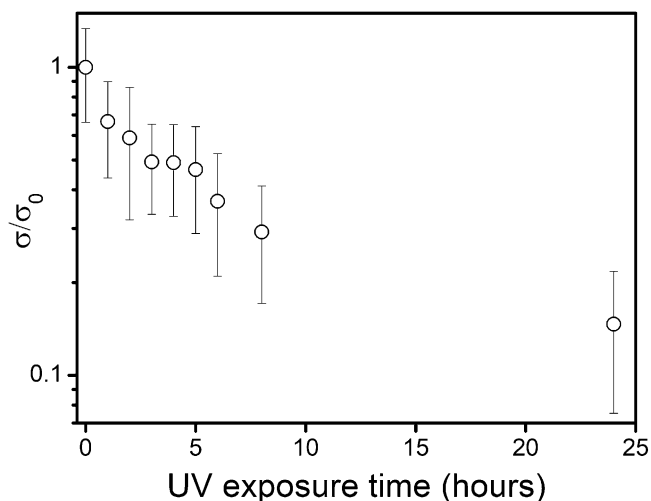


Fig. 4 Change in conductivity of MXene film with increasing UV exposure time

the original value on the 29th day and 4% of the original value by the 50th day. Similar to the $\text{Ti}_3\text{C}_2\text{T}_x$ film in air, there seems to be a strong decrease in conductivity within the first 4 weeks, followed by a more gradual decrease in conductivity thereafter (seen in detail in Fig. 3). This indicates a slowdown in the oxidation of $\text{Ti}_3\text{C}_2\text{T}_x$, most likely due to the decreasing number of reactive sites with time. Note that the two polymer composite samples (regardless of the amount of polymer) and the $\text{Ti}_3\text{C}_2\text{T}_x$ film in air sample follow a similar trend. This suggests that the mechanism of oxidation in polymer composite is not affected by the amount of polymer, and the hydrophilic polymer does not form an effective protective barrier to prevent oxidation.

These findings are consistent with the observations made on our recently reported layer-by-layer (LbL) films.²³ Over a course of 4 weeks, the absorbance of these MXene/PDAC LbL films decreased, suggesting oxidation (Supplementary Fig. S9).

We also examined oxidation under UV irradiation. In previous studies, $\text{Ti}_3\text{C}_2\text{T}_x$ dispersions have demonstrated a strong absorbance in the wavelength range of 250–300 nm.¹¹ Therefore, we hypothesized that the exposure of $\text{Ti}_3\text{C}_2\text{T}_x$ to UV light in this wavelength range would accelerate oxidation. Based on our data (Fig. 4 and Supplementary Table S1), there is a strong downtrend in conductivity with a longer UV time exposure, suggesting an increase in oxidation. It took only 24 h of UV exposure under

atmospheric conditions to cause a conductivity loss of over > 85%, while a similar sample under atmospheric conditions and stored in relative darkness experienced a conductivity loss of over > 85% in 27 days. This has serious implications for $\text{Ti}_3\text{C}_2\text{T}_x$ MXene composites made from UV-cured polymers; UV curing may degrade $\text{Ti}_3\text{C}_2\text{T}_x$ MXenes within the monomer.

We argue that there are two reasons for the accelerated $\text{Ti}_3\text{C}_2\text{T}_x$ oxidation under UV light. The first is the transformation of UV light to heat, leading to an increased oxidation kinetics. It has been demonstrated that $\text{Ti}_3\text{C}_2\text{T}_x$ MXenes can absorb light and convert it to heat with almost 100% efficiency.³⁶ The second is the generation of radicals under UV light that may attack the $\text{Ti}_3\text{C}_2\text{T}_x$ surface, causing further oxidation. We surmise that the UV light interacts with the TiO_2 causing O^\cdot and OH^\cdot radical formation from the oxygen and moisture present in the environment.³⁷ With longer UV exposure times, more radicals were generated, leading to more oxidation. Even so, more experiments need to be done to properly assess UV effects on $\text{Ti}_3\text{C}_2\text{T}_x$ oxidation.

DISCUSSION

We assessed $\text{Ti}_3\text{C}_2\text{T}_x$ oxidation behavior in air, liquid, and solid media; we observed that the oxidation is the slowest in solid media and the fastest in liquid media. In water, $\text{Ti}_3\text{C}_2\text{T}_x$ oxidizes within 2 weeks, and the data suggest that the dispersion's black color and colloidal stability are not reliable indicators of oxidation, contrary to the prior reports. From a storage perspective, $\text{Ti}_3\text{C}_2\text{T}_x$ can be preserved in ice (and to a lesser extent in some organic solvents) to decrease oxidation or freeze dried to form a re-dispersible powder. $\text{Ti}_3\text{C}_2\text{T}_x$ composites, regardless of the amount of polymer, display similar profiles in terms of decrease in conductivity, suggesting that the polymer does not act as a barrier to decrease oxidation. Additionally, we have found that exposure to UV accelerates oxidation in $\text{Ti}_3\text{C}_2\text{T}_x$ films. We anticipate that this will be one of the many studies needed within the MXene community to understand and prevent their oxidation and allow for their longer shelf life and reliable functional properties.

METHODS

Synthesis of Ti_3AlC_2 MAX phase

Commercial Ti (average particle size 44 μm , 99.5% purity), Al (average particle size 44 μm , 99.5% purity), and TiC powders (average particle size 2–3 μm , 99.5% purity) (all from Alfa Aesar, MA, USA) were used as starting raw materials to synthesize Ti_3AlC_2 MAX phase. To prepare homogeneous powder mixtures, Ti, Al, and TiC powders were first weighed to achieve Ti:Al:C = 3.0:1.2:1.8 ratio and mixed together using ball milling with zirconia beads in a glass jar at a speed of 300 rpm for 24 h. Then, the bulk high-purity Ti_3AlC_2 samples were sintered at a temperature of 1510 $^\circ\text{C}$ for 15 min with a loading of 50 MPa using Pulsed Electric Current System (PECS). To fabricate high-purity Ti_3AlC_2 powder, the PECSed sample was first drill milled and sieved to obtain powder with particle sizes below 44 μm .¹¹

Synthesis of $\text{Ti}_3\text{C}_2\text{T}_x$ MXene clay

$\text{Ti}_3\text{C}_2\text{T}_x$ MXene clay was synthesized by etching Al from the Ti_3AlC_2 phase using the technique described by Ghidui et al.³⁸ Concentrated hydrochloric acid (HCl, ACS reagent, 37% w/w; Sigma-Aldrich) was diluted with DI water to obtain 30 ml of 6 M HCl solution. This solution was transferred to a polypropylene (PP) beaker and 1.98 g of lithium fluoride (LiF, 98 + % purity; Alfa Aesar) was added to it. This dispersion was stirred for 5 min using a polytetrafluoroethylene magnetic stirrer at room temperature. Ti_3AlC_2 MAX phase powder was slowly added to the HCl + LiF solution to prevent overheating as the reaction is exothermic. The PP beaker was capped to prevent the evaporation of water, and a hole was made in the cap to avoid the buildup of hydrogen gas. The reaction mixture was stirred at 40 $^\circ\text{C}$ for about 45 h. The slurry product was centrifuged and washed with DI water to remove the unreacted hydrofluoric acid and water-soluble salts. This washing process was repeated until the pH of the filtrate reached a value of about 5. The reaction product was collected at the

bottom of the PP centrifuge tubes and was extracted as $\text{Ti}_3\text{C}_2\text{T}_x$ MXene clay.¹¹

Intercalation and delamination of $\text{Ti}_3\text{C}_2\text{T}_x$ MXene clay

$\text{Ti}_3\text{C}_2\text{T}_x$ MXene clay was intercalated with DMSO and eventually bath sonicated to obtain an aqueous dispersion of delaminated $\text{Ti}_3\text{C}_2\text{T}_x$ MXenes following the procedure described in more detail by Mashtalir et al.⁷ DMSO (ReagentPlus, >99.5%; Sigma-Aldrich) was added to $\text{Ti}_3\text{C}_2\text{T}_x$ MXene to form a 60 mg/ml suspension followed by about 18 h of stirring at room temperature. After intercalation, the excess DMSO was removed by several cycles of washing with DI water and centrifugation at 5000 rpm for 4 h. The suspension of intercalated $\text{Ti}_3\text{C}_2\text{T}_x$ MXene clay in deionized water was bath sonicated for 1 h at room temperature followed by centrifugation at 3500 rpm for 1 h to separate the heavier components.¹¹

Preparation of $\text{Ti}_3\text{C}_2\text{T}_x$ vacuum-filtered film before freeze drying

After centrifugation, the supernatant was collected and vacuum filtered on a polytetrafluoroethylene membrane (0.45- μm pore size). The vacuum-filtered film was then vacuum dried overnight. This was the reference for all vacuum-filtered samples.

Freeze drying $\text{Ti}_3\text{C}_2\text{T}_x$ nanosheets

After centrifugation, the collected supernatant was stored in a freezer (<0 °C) and then freeze dried (Labconco FreeZone) for 3 days to obtain $\text{Ti}_3\text{C}_2\text{T}_x$ nanosheet powder.

$\text{Ti}_3\text{C}_2\text{T}_x$ in organic solvent

The freeze-dried $\text{Ti}_3\text{C}_2\text{T}_x$ powder was added to 100 ml of acetone and acetonitrile at a concentration of 1 mg ml⁻¹. $\text{Ti}_3\text{C}_2\text{T}_x$ powder in both the organic solvents was mixed with the aid of a vortex mixer to form a temporary colloidal solution as all the $\text{Ti}_3\text{C}_2\text{T}_x$ powder sedimented out after a few minutes (for both acetone and acetonitrile). Therefore, to obtain a vacuum-filtered film, the solution was vacuum filtered right after vortex mixing. The vacuum-filtered film was then vacuum dried (to eliminate any moisture) before the conductivity was measured.

$\text{Ti}_3\text{C}_2\text{T}_x$ in water

The $\text{Ti}_3\text{C}_2\text{T}_x$ powder (concentration of 1 mg ml⁻¹) was added to 100 ml of water and shaken with the aid of a vortex mixer; the powder dispersed upon contact with water. Ten milliliters of the sample was drawn out every week to prepare a vacuum-filtered film. The film was then vacuum dried overnight (room temperature) before its electrical conductivity was measured.

$\text{Ti}_3\text{C}_2\text{T}_x$ in ice

Forty milliliters from the water dispersion was drawn out and separated into four 10 ml samples. The four samples were stored in the freezer to freeze the samples. To prepare a film to measure the electrical conductivity, each sample was thawed by submerging the sample container in room-temperature water. After thawing, the sample was vacuum filtered to obtain a film; the film was then vacuum dried overnight before its electrical conductivity was measured.

$\text{Ti}_3\text{C}_2\text{T}_x$ in polymers

$\text{Ti}_3\text{C}_2\text{T}_x$ powder and PVA (one sample with 50–50wt% and another with 10–90 wt%, respectively, with a total solid concentration of 1 mg ml⁻¹) were bath sonicated for 15 min and then vacuum filtered to obtain a polymer composite film. These films were vacuum dried overnight (room temperature) before their electrical conductivity was measured.

UV oxidation

$\text{Ti}_3\text{C}_2\text{T}_x$ dispersion was vacuum filtered for 30 min to obtain a buckypaper film and then it was vacuum oven dried overnight to remove all moisture. Conductivity of the $\text{Ti}_3\text{C}_2\text{T}_x$ film was measured before and after UV exposure. All the experiments were done under dark housing, where the only source of light the sample was exposed to was the UV lamp (254 nm, 4W, 0.16A).

Characterization

Conductivity measurements were done using 4-Point Resistivity Probe powered by Keithley 2000, 6221, and two 6514s. XPS measurements were conducted using Omnicron XPS. Zeta potential was measured using Malvern Zetasizer ZS90. UV–vis measurements were done using Shimadzu UV–vis 2550.

DATA AVAILABILITY

All the data generated and analyzed in this study are included in this manuscript and its supplementary information file. Additional details are available upon request.

ACKNOWLEDGEMENTS

Funding for the study was provided by the US National Science Foundation (Grant No. CMMI-1760859) and TAMU Energy institute. We would like to acknowledge the use of the TAMU Materials Characterization Facility and TAMU Microscopy & Imaging Center. We would also like to acknowledge Dr. Mustafa Akbulut of TAMU for allowing us to use his group's ZetaSizer instrument for zeta potential measurements.

AUTHOR CONTRIBUTIONS

T.H. and X.Z. prepared the samples, designed and performed the experiments, and analyzed the data. S.S. and Y.C. assisted with the synthesis and etching of Ti_3AlC_2 MAX phase. W.S. assisted with SEM. H.A. assisted with UV–vis measurements of LbL films. J.L.L., M.R., and M.J.G. provided guidance and assisted with the designing of experiments, data analysis, and writing of the manuscript.

ADDITIONAL INFORMATION

Supplementary information accompanies the paper on the *npj 2D Materials and Applications* website (<https://doi.org/10.1038/s41699-019-0089-3>).

Competing interests: The authors declare no competing interests.

Publisher's note: Springer Nature remains neutral with regard to jurisdictional claims in published maps and institutional affiliations.

REFERENCES

- Naguib, M. et al. Two-Dimensional nanocrystals produced by exfoliation of Ti_3AlC_2 . *Adv. Mater.* **23**, 4248–4253 (2011).
- Anasori, B. et al. Two-Dimensional, Ordered, Double Transition Metals Carbides (MXenes). *ACS Nano* **9**, 9507–9516 (2015).
- Sun, W. et al. Electrochemical etching of Ti_2AlC to Ti_2CT_x (MXene) in low-concentration hydrochloric acid solution. *J. Mater. Chem. A* **5**, 21663–21668 (2017).
- Naguib, M. et al. Two-Dimensional Transition Metal Carbides. *ACS Nano* **6**, 1322–1331 (2012).
- Shahzad, F. et al. Electromagnetic interference shielding with 2D transition metal carbides (MXenes). *Science* **353**, 1137–1140 (2016).
- Han, M. et al. Ti_3C_2 MXenes with Modified Surface for High-Performance Electromagnetic Absorption and Shielding in the X-Band. *ACS Appl. Mater. & Interfaces* **8**, 21011–21019 (2016).
- Mashtalir, O. et al. Intercalation and delamination of layered carbides and carbonitrides. *Nat. Commun.* **4**, 1716 <https://www.nature.com/articles/ncomms2664#supplementary-information> (2013).
- Er, D., Li, J., Naguib, M., Gogotsi, Y. & Shenoy, V. B. Ti_3C_2 MXene as a high capacity electrode material for metal (Li, Na, K, Ca) ion batteries. *ACS Appl. Mater. & Interfaces* **6**, 11173–11179 (2014).
- Hu, M. et al. Self-assembled $\text{Ti}_3\text{C}_2\text{T}_x$ MXene film with high gravimetric capacitance. *Chem. Commun.* **51**, 13531–13533 (2015).
- Zhang, H. et al. Preparation, mechanical and anti-friction performance of MXene/polymer composites. *Mater. & Des.* **92**, 682–689 (2016).
- Shah, S. A. et al. Template-free 3D titanium carbide ($\text{Ti}_3\text{C}_2\text{T}_x$) MXene particles crumpled by capillary forces. *Chem. Commun.* **53**, 400–403 (2017).
- Hu, Q. et al. MXene: A New Family of Promising Hydrogen Storage Medium. *J. Phys. Chem. A* **117**, 14253–14260 (2013).
- Rasool, K. et al. Antibacterial Activity of $\text{Ti}_3\text{C}_2\text{T}_x$ MXene. *ACS Nano* **10**, 3674–3684 (2016).
- Ling, Z. et al. Flexible and conductive MXene films and nanocomposites with high capacitance. *Proc. Natl Acad. Sci.* **111**, 16676–16681 (2014).

15. Ren, C. E. et al. Charge- and Size-Selective Ion Sieving Through $\text{Ti}_3\text{C}_2\text{Tx}$ MXene Membranes. *J. Phys. Chem. Lett.* **6**, 4026–4031 (2015).
16. Guo, J. et al. Theoretical interpretation on lead adsorption behavior of new two-dimensional transition metal carbides and nitrides. *J. Alloy. Compd.* **684**, 504–509 (2016).
17. Luo, J. et al. Sn^{4+} Ion Decorated Highly Conductive Ti_3C_2 MXene: Promising Lithium-Ion Anodes with Enhanced Volumetric Capacity and Cyclic Performance. *ACS Nano* **10**, 2491–2499 (2016).
18. Levi, M. D. et al. Solving the Capacitive Paradox of 2D MXene using Electrochemical Quartz-Crystal Admittance and In Situ Electronic Conductance Measurements. *Adv. Energy Mater.* **5**, 1400815–1401400 (2015).
19. Luo, J. et al. Pillared Structure Design of MXene with Ultralarge Interlayer Spacing for High-Performance Lithium-Ion Capacitors. *ACS Nano* **11**, 2459–2469 (2017).
20. Wang, R. et al. Graphene-coupled Ti_3C_2 MXenes-derived TiO_2 mesostructure: promising sodium-ion capacitor anode with fast ion storage and long-term cycling. *J. Mater. Chem. A* **6**, 1017–1027 (2018).
21. Tang, Q., Zhou, Z. & Shen, P. Are MXenes Promising Anode Materials for Li Ion Batteries? Computational Studies on Electronic Properties and Li Storage Capability of Ti_3C_2 and $\text{Ti}_3\text{C}_2\text{X}_2$ ($\text{X} = \text{F}, \text{OH}$) Monolayer. *J. Am. Chem. Soc.* **134**, 16909–16916 (2012).
22. Sun, D. et al. *Two-Dimensional Ti_3C_2 as Anode Material for Li-Ion Batteries*. Vol. 47 (2014).
23. An, H. et al. Surface-agnostic highly stretchable and bendable conductive MXene multilayers. *Science Advances* **4** <https://doi.org/10.1126/sciadv.aag0118> (2018).
24. Ghassemi, H. et al. In situ environmental transmission electron microscopy study of oxidation of two-dimensional Ti_3C_2 and formation of carbon-supported TiO_2 . *J. Mater. Chem. A* **2**, 14339–14343 (2014).
25. Halim, J. et al. X-ray photoelectron spectroscopy of select multi-layered transition metal carbides (MXenes). *Appl. Surf. Sci.* **362**, 406–417 (2016).
26. Maleski, K., Mochalin, V. N. & Gogotsi, Y. Dispersions of Two-Dimensional Titanium Carbide MXene in Organic Solvents. *Chem. Mater.* **29**, 1632–1640 (2017).
27. Zhang, C. J. et al. Oxidation Stability of Colloidal Two-Dimensional Titanium Carbides (MXenes). *Chem. Mater.* **29**, 4848–4856 (2017).
28. Ghidui, M., Lukatskaya, M. R., Zhao, M.-Q., Gogotsi, Y. & Barsoum, M. W. Conductive two-dimensional titanium carbide ‘clay’ with high volumetric capacitance. *Nature* **516**, 78 (2014).
29. Ju, Y., Wang, M., Wang, Y., Wang, S. & Fu, C. Electrical properties of amorphous titanium oxide thin films for bolometric application. *Adv. Condens. Matter Phys.* **2013**, 5 (2013).
30. Marcano, D. C. et al. Improved synthesis of graphene oxide. *ACS Nano* **4**, 4806–4814 (2010).
31. Jung, I., Dikin, D. A., Piner, R. D. & Ruoff, R. S. Tunable Electrical Conductivity of Individual Graphene Oxide Sheets Reduced at “Low” Temperatures. *Nano. Lett.* **8**, 4283–4287 (2008).
32. Romer, F. M. et al. Controlling the conductivity of Ti_3C_2 MXenes by inductively coupled oxygen and hydrogen plasma treatment and humidity. *RSC Adv.* **7**, 13097–13103 (2017).
33. Ghidui, M. et al. Ion-Exchange and Cation Solvation Reactions in Ti_3C_2 MXene. *Chem. Mater.* **28**, 3507–3514 (2016).
34. Sobolciak, P. et al. 2D $\text{Ti}_3\text{C}_2\text{T}(\text{x})$ (MXene)-reinforced polyvinyl alcohol (PVA) nanofibers with enhanced mechanical and electrical properties. *PLoS One* **12**, e0183705 (2017).
35. Hallensleben, M. L. Polyvinyl Compounds, Others. In *Ullmann's Encyclopedia of Industrial Chemistry*. (Ed.). https://doi.org/10.1002/14356007.a21_743 (2000).
36. Li, R., Zhang, L., Shi, L. & Wang, P. MXene Ti_3C_2 : An Effective 2D Light-to-Heat Conversion Material. *ACS Nano* **11**, 3752–3759 (2017).
37. Hiraoka, T. & Nosaka, Y. Properties of O_2^- and OH^\bullet Formed in TiO_2 Aqueous Suspensions by Photocatalytic Reaction and the Influence of H_2O_2 and Some Ions. *Langmuir* **18**, 3247–3254 (2002).
38. Ghidui, M., Lukatskaya, M. R., Zhao, M.-Q., Gogotsi, Y. & Barsoum, M. W. Conductive two-dimensional titanium carbide/clay with high volumetric capacitance. *Nature* **516**, 78–81 (2014).



Open Access This article is licensed under a Creative Commons Attribution 4.0 International License, which permits use, sharing, adaptation, distribution and reproduction in any medium or format, as long as you give appropriate credit to the original author(s) and the source, provide a link to the Creative Commons license, and indicate if changes were made. The images or other third party material in this article are included in the article's Creative Commons license, unless indicated otherwise in a credit line to the material. If material is not included in the article's Creative Commons license and your intended use is not permitted by statutory regulation or exceeds the permitted use, you will need to obtain permission directly from the copyright holder. To view a copy of this license, visit <http://creativecommons.org/licenses/by/4.0/>.

© The Author(s) 2019